Intrinsic radial sensitivity of nucleon inelastic scattering

J. J. Kelly
Department of Physics and Astronomy, University of Maryland, College Park, Maryland 20742
(Received 14 November 1986)

A linear expansion analysis of the folding model transition amplitude is used to study the intrinsic sensitivity of the inelastic scattering of intermediate energy nucleons to the radial form of the neutron transition density, given known proton transition densities from electron scattering. Realistic density-dependent effective interactions are used to construct pseudodata. These pseudodata are then reanalyzed and the error matrix is used to calculate an error band for the radial transition density. This approach reveals the sensitivity of the extracted transition density to absorption, medium modifications of the interaction, and the extent and quality of the data in a manner that is largely free of the residual inaccuracies in reaction theory that complicate the analysis of real data. We find that the intrinsic radial sensitivity of nucleon inelastic scattering is best for projectile energies between 200 and 500 MeV, but is adequate to resolve the radial dependence of neutron transition densities even in the interior of heavy nuclei throughout the energy regime 100–800 MeV. We have also compared our method with scale-factor analyses which assume proportionality between neutron and proton densities. For states whose transition densities are similar in the surface, we find scaling to be accurate at the 20% level. However, for light nuclei substantial deviations beyond the first peak of the differential cross section reveal sensitivity to shape differences. This sensitivity is reduced for heavy nuclei. The model dependence of radial densities is also studied. A high-q constraint is used to analyze the contribution of incompleteness error to the deduced error bands and to reduce the model dependence.

I. INTRODUCTION

Electroexcitation of discrete nuclear transitions has become firmly established as a quantitative probe of the radial structure of nuclei and provides radial transition charge densities with excellent precision.[1] These precise measured densities constitute a very stimulating and rigorous challenge to theories of nuclear structure.[2] However, electrons are essentially blind to half of the nuclear constituents, viewing neutrons almost exclusively through the magnetic moment of a single unpaired valence neutron.[3] Therefore, the development of a quantitative technique to measure radial transition densities for neutrons represents an important challenge to nuclear physics.

Hadronic probes, on the other hand, are about equally sensitive to neutron and protons. However, uncertainties in the reaction mechanism often confound the interpretation of data for hadron scattering. Therefore, most analyses are content to extract a simple scale-factor that characterizes the relative contributions of neutrons and protons in a qualitative manner. This procedure is most applicable to low-lying collective excitations for which it is reasonable to assume that the shapes of the neutron and proton transition densities are similar in the surface region. Many such studies have been performed. For example, a series of papers by Bernstein *et al.* has reviewed the ratio of neutron and proton matrix elements, M_n/M_p, for low-lying collective excitations that were extracted from data for a variety of reactions.[4–6] They find that the various analyses yield general consistency at the 20% level.

However, except in the lowest collective states, the radial shapes of neutron and proton transition densities will often be considerably different. Whereas collective core excitations are predominantly isoscalar, the differences between neutron and proton transition densities reveal the specific valence orbitals involved. Even in the lowest collective states, the ratio between neutron and proton matrix elements is often considerably different from the simple N/Z prediction of the hydrodynamic model.[4] A comprehensive survey of such transitions has recently been performed by Lombard and Mas,[7] who use the energy density method to supplement the shell model with semiempirical coupling to giant resonances. This model achieves good global agreement with measured reduced transition probabilities. Good agreement has also been demonstrated for several transition charge densities. This theory predicts dramatic differences between neutron and proton densities, in shape as well as in scale. Even larger differences are expected for higher-lying excitations. Equally important shape differences for *sd*-shell nuclei have also been predicted by Brown, Radhi and Wildenthal.[8]

Experimental information about the radial shape of neutron transition densities is of fundamental importance to the evaluation of microscopic theories of nuclear structure. Yet, there are few reliable measurements of shape differences between neutron and proton transition densities. The purpose of this paper is to evaluate the intrinsic sensitivity of nucleon scattering to the radial form of the neutron transition density.

We have developed a versatile modeling procedure based on a linear expansion of the transition amplitude in the folding model.[9–13] Such a transition amplitude may be described by the schematic "$t\rho$" form representing the convolution of an effective interaction t with a nuclear transition density ρ. For states whose relevant nuclear structure variables are accurately known from a reliable source, such as electron scattering, the medium modifications of the effective interaction can be expanded in a linear series about a suitable initial value and optimized with respect to a large body of data.[14] Having established an empirical effective interaction, the structure of states for which only a single radial density is unknown may be determined by expanding the radial dependence in a suitable basis and fitting the coefficients to data for any set of reactions which share this common density.

This procedure is almost model independent in the sense that any plausible radial variation can be represented by a small set of suitable basis functions. The interpretation of data is then unbiased by the choice of model.

Ground-state neutron densities have been studied using similar "*model-independent*" analyses of high-energy proton scattering.[15] The accuracy of these results has been studied using the dependence of the fitted densities upon projectile energy. Unfortunately, the degree of consistency obtained in these studies is usually not sufficient to confidently interpret the relatively small differences in radial shape between ground-state neutron and proton densities. Related work with alphas[16] and pions[11,17] presents similar difficulties. However, given the dramatic differences between the predicted shapes of neutron and proton transition densities, we expect inelastic scattering to offer larger and more varied signals than elastic scattering. We may then expect to learn significant new nuclear structure information even while using an imperfect reaction theory. Therefore, nucleon inelastic scattering presents more favorable opportunities.

To establish the inelastic scattering of intermediate energy nucleons as a quantitative probe of neutron transition densities, three primary issues must be addressed. First, we should investigate the intrinsic radial sensitivity the probe could achieve if the reaction theory were perfectly accurate. Second, we must understand the dependence of our results upon the choice of model used to represent the density. Finally, we must ascertain the accuracy of our results by investigating their sensitivity to residual errors in the theory used to describe the reaction. The present paper addresses the issues of sensitivity and model dependence, leaving the question of accuracy to future publications.

Our method for modeling inelastic scattering is presented in Sec. II. The intrinsic radial sensitivity of nucleon inelastic scattering is studied in Sec. III using pseudodata to minimize residual inaccuracies in reaction theory. Our method is compared to traditional scaling analyses in Sec. III C. The dependence of the fitted density upon the unmeasured region of large momentum transfer is studied in Sec. IV by adapting an analysis of incompleteness error developed for electron scattering. Finally, our conclusions are presented in Sec. V.

II. MODELING INELASTIC SCATTERING

A. Linear expansion analysis

We represent the scattering amplitude T for the binary reaction $A(\vec{a},\vec{b})B$ as a linear expansion

$$T=\sum a_n T^n(\theta) \tag{1}$$

of coefficients a_n times basis amplitudes $T^n(\theta)$, where the four spin projections (m_A,m_a,m_b,m_B) have been suppressed for clarity. The quadratic forms

$$X^{nn'}_{\alpha\beta}(\theta)=\mathrm{Tr}[T^n(\theta)\sigma_\alpha T^{n'}(\theta)^*\sigma_\beta] \tag{2}$$

are then constructed as traces over spin projections of products involving the basis amplitudes and the polarization vectors σ_α and σ_β. The polarization vectors are simply Pauli matrices for nucleons. The observables are then contractions of these quadratic forms:

$$\sigma_0(\theta)=\frac{\mu_a\mu_b}{(2\pi)^2}\frac{k_b}{k_a}I_0(\theta)\ , \tag{3a}$$

$$I_0(\theta)=\tfrac{1}{2}\sum_{nn'} a_n X^{nn'}_{00}(\theta)a^*_{n'}\ , \tag{3b}$$

$$I_0 D_{\alpha\beta}=\tfrac{1}{2}\sum_{nn'} a_n X^{nn'}_{\alpha\beta}(\theta)a^*_{n'}\ , \tag{3c}$$

where μ_a (μ_b) is the reduced mass and k_a (k_b) is the wave number in the incident (exit) channel. The analyzing power $A_y=D_{y0}$ and the induced polarization $P=D_{0y}$ are special cases of the depolarization matrix $D_{\alpha\beta}$ defined by Ohlsen.[18]

A very simple search algorithm can be used to minimize the total chi-square (χ^2) for an arbitrary set of observables with respect to the expansion coefficients a_n. The method is efficient in the sense that the basis amplitudes need only be calculated once and then stored—it is not necessary to recalculate distorted waves or overlap integrals during the optimization of parameters. In fact, whenever the excitation energy is a negligible fraction of the incident energy, all states of the same multipolarity in a given target nucleus can share a common set of basis amplitudes. The method is versatile in that it is applicable to any structure or interaction model that can be represented by a linear expansion.

Although our applications have been restricted to inelastic scattering within a nonrelativistic distorted wave approximation that uses local operators, the method itself is more general and is equally applicable to nonlocal interactions or to relativistic theories. All that is really required is that the reaction be direct and that the transition amplitude can be linearized with respect to the quantity of interest. It just happens that the nonrelativistic theory is, at present, more highly developed and more convenient to use. Furthermore, these methods can be easily extended to elastic scattering and to iterative cycles in which the distortion is varied self-consistently.

B. Folding model

Reaction models of the folding type are most amenable to a linear expansion analysis (LEA). While these models may differ greatly in detail, all folding models may be described by the schematic "$t\rho$" form representing the convolution of an effective interaction t with a nuclear transition density ρ. Control of either the structure or interaction factor permits the systematic investigation of the unknown factor within a linear expansion analysis.

The states of interest to the present investigation are normal parity transitions whose transverse form factors for electroexcitation are demonstrably small over the entire range of momentum transfer below 2.7 fm^{-1}. The spin and current contributions are then negligible. We also assume that other currents relevant to nucleon scattering are also negligible.[19] These conditions are satisfied most accurately by relatively collective transitions.

For these transitions, the scattering potential

$$U(\mathbf{r})=U^C-\nabla U^{LS}\otimes\frac{1}{i}\nabla\cdot\sigma \tag{4}$$

can be expanded in multipoles with radial potentials of the form

$$U_J^C(r)=\frac{2}{\pi}\int dq\, q^2 j_J(qr)\sum_\lambda \tilde{t}_{0\lambda}^C(q,\rho)\rho_{J\lambda}(q)\ , \tag{5a}$$

$$U_J^{LS}(r)=\frac{2}{\pi}\int dq\, q^2 j_J(qr)\sum_\lambda \tilde{t}_\lambda^{LS}(q,\rho)\rho_{J\lambda}(q)\ , \tag{5b}$$

where λ=p (n) for proton (neutron) or 0 (1) for isoscalar (isovector). For simplicity, the density dependence of the central and spin-orbit interactions $\tilde{t}^C$ and $\tilde{t}^{LS}$ is evaluated at the site of the projectile. Knock-on exchange is included in the zero-range approximation.[20] More complete descriptions of the reaction model may be found in Refs. 21–23.

For energies $E_p\le 400$ MeV, we employed a density-dependent effective interaction based on the Paris potential.[24,25] For $E_p\ge 500$ MeV, the Love-Franey parametrization of the free t matrix was used.[26] Microscopic optical potentials were employed throughout. These potentials were obtained by folding the same effective interactions with the ground-state density, assuming $\rho_n\propto\rho_p$. Ground-state densities were constructed by unfolding the proton form factor from charge densities tabulated by de Vries *et al.*[27]

C. Radial densities

A radial density $\rho_l(r)$ can be represented as a linear expansion,

$$\rho_l(r)=\sum_\nu a_\nu f_{\nu l}(r)\ , \tag{6}$$

where the radial basis functions $f_{\nu l}(r)$ are drawn from any convenient complete set. The expansion coefficients a_ν can be fitted by minimizing the composite χ^2 for all available data. The error envelope can then be deduced from the error matrix. This type of analysis is almost model independent in the sense that rather than fitting with a restrictive, and arbitrary, analytic form, the significant coefficients of an expansion in a complete basis of radial functions are fitted. The resulting density is then not biased by the choice of model. Virtually any radial function can be represented in this manner, with only minor restrictions being imposed by the inevitable truncation of the series.

The transition amplitude is conveniently represented by the matrix element

$$M_\lambda=\int dr\, r^{l+2}\rho_{l\lambda}(r)\ , \tag{7}$$

where λ=n or p. For comparisons with electroexcitation data it is convenient to define the form factor for transitions between nuclear states with initial and final spins J_i and J_f as

$$F_\lambda(q)=\left[\frac{4\pi}{N_\lambda}\right]^{1/2}\frac{\hat{J}_f}{\hat{J}_i}\tilde{\rho}_l(q)\ , \tag{8}$$

where

$$\tilde{\rho}_l(q)=\int dr\, r^2 j_l(qr)\rho_l(r)=\sum_\nu a_\nu\tilde{f}_{\nu l}(q) \tag{9}$$

is the Fourier-Bessel transform of the transition density and where $\hat{x}=\sqrt{2x+1}$. The particle number N_λ is either N or Z according to whether λ=n or p. In the plane-wave approximation, the cross section for nucleon scattering is proportional to the square of the form factor and to an elementary cross section.[14]

Electron scattering data are most often analyzed using some variation of the Fourier-Bessel expansion[1,28] (FBE),

$$f_{\nu l}(r)=\begin{cases} j_l(q_\nu r), & r\le R \\ 0, & r\ge R. \end{cases} \tag{10}$$

The principal advantage of this expansion of this expansion is that the dominant contribution each term ν makes to the form factor is localized near its characteristic momentum transfer q_ν, such that

$$\tilde{f}_{\nu l}(q)=\frac{q_\nu R^2}{q_\nu^2-q^2}j_l(qR)j_{l+1}(q_\nu R)\ \ (q\neq q_\nu)\ , \tag{11a}$$

$$\tilde{f}_{\mu l}(q_\nu)=\frac{R^3}{2}j_{l+1}^2(q_\nu R)\delta_{\mu\nu}\ . \tag{11b}$$

Thus, only one term of the FBE contributes at each characteristic momentum q_ν. While other expansions are useful, none has a relationship between its expansion coefficients and the form factor that is so transparent. If the plane-wave approximation were accurate, the expansion coefficients could be determined directly from measurements performed at $q=q_\nu$ for each $\nu=1,\ldots,N$ such that $N+l/2\lesssim q_m R/\pi$, where q_m is the maximum momentum transfer accessible to measurement.

A significant defect of the FBE is that each basis function is oscillatory at large radius. Thus, unless sufficient data exist at small momentum transfer or unless the asymptotic radial behavior is suitably biased, undesirable oscillations will persist at unreasonably large radii.

The polynomial-Gaussian expansion (PGE),

$$f_{vl}(r)=(\alpha^3 y^l e^{-y^2})y^{2v} , \tag{12}$$

where $y=\alpha r$, provides a useful alternative with a set of advantages and disadvantages complementary to that of the FBE. The PGE decreases exponentially for both large radius and large momentum transfer. If α is chosen according to the harmonic oscillator model, a natural radial scale is introduced which minimizes the number of coefficients required to represent any plausible radial variation. However, the form factors for each basis function are not localized in momentum transfer. Moreover, the radial basis functions overlap strongly, causing the fitted coefficients to be highly correlated.

A third alternative can be found in the Laguerre-Gaussian expansion[29] (LGE),

$$f_{vl}(r)=x^l e^{-x^2} L_v^{l+1/2}(2x^2) , \tag{13}$$

where $x=r/b$ and L_v^a is a generalized Laguerre polynomial. This expansion also enjoys exponential decay at both large radius and large momentum transfer. The oscillator parameter b establishes a natural radial scale. However, as an orthogonal series, the correlation between adjacent coefficients is considerably less than that which plagues the PGE.

III. INTRINSIC RADIAL SENSITIVITY

A. Pseudodata method

The intrinsic radial sensitivity of nucleon inelastic scattering can be studied in a manner that is essentially independent of residual inaccuracies in the reaction model. The basic premise is that the present reaction theory is sufficiently accurate to assess, at least qualitatively, the effects of absorption and of density dependence in the effective interaction upon the extraction of neutron transition densities from the data. The impact of residual inaccuracies is minimized by using a pseudodata approach. Representative structure models are used to calculate scattering observables within the present theoretical framework. As the proton density is usually taken from electron scattering, the range of momentum transfer is restricted to that which is generally measured in such experiments. In practice, these measurements usually extend a little beyond twice the Fermi momentum because higher momentum components are not expected to be very important. The number of points within this range should reflect experimental practice. Pseudodata are then constructed by applying random fluctuations, using a random number generator, according to a normal distribution whose width reflects customary experimental precision. Similar methods have been used to study the scattering of electrons,[28,30] pions,[11] and kaons.[31]

The neutron transition density is then fitted to this set of pseudodata, holding the proton density fixed. The error band on the neutron density is then calculated from the full error matrix for the fit, including the correlations among parameters. The fitted densities tend to be distributed within this error band and chi-square tends to be distributed normally about unity because the reaction model is perfect by construction. Using a sample consisting of many independent pseudodata trials, we have, in fact, explicitly demonstrated that the sample mean and variance converge to the input density and error envelope, respectively. Thus, the original input density is recovered with an estimate of the ideal minimum uncertainty with which the density can be determined at all radii. In analyzing real data, however, additional uncertainties arise from uncertainties in the reaction theory.

The present estimate of the error envelope includes, implicitly, contributions from several sources. First, the precision, range, and number of data determine the minimum uncertainty with which a density can be extracted assuming a transparent medium without distortion. This situation corresponds closely to that realized for electron scattering. Second, absorption reduces the contribution of the interior of the nucleus and thus expands the error envelope in the interior. Third, Pauli blocking reduces the strength of the effective interaction in the interior and thus also inhibits scattering from the interior.

The experimental precision achieved by proton scattering experiments is often better than a few percent. Unfortunately, we cannot expect comparable accuracy from reaction theory. This is perhaps responsible for the fact that our analysis of real data rarely produces reduced chi-squares near unity despite the flexibility available in the parametrization of the radial density. Thus, in practice, we fold an additional $\pm 10\%$ relative uncertainty into the estimated uncertainty of measured cross sections. Therefore, our pseudodata will also be constructed with error bars of $\pm 10\%$, thereby implicitly recognizing the limitations imposed by our less than ideal reaction theory. When this additional uncertainty is omitted, the estimated error bands become unrealistically tight, as narrow as those from electron scattering. Such was the case in the neutron transition density for the lowest 2^+ state of ^{18}O that we recently published.[13]

B. Interior sensitivity: Monopole transitions

Inelastic monopole transitions provide the best insight into the intrinsic radial sensitivity of nucleon inelastic scattering. The transition densities for higher multipolarities, $l>0$, must behave as r^l near the origin. Therefore, both the density and its uncertainty vanish at the origin in a manner that is representative of the multipolarity, rather than of the interior sensitivity of the probe. Monopole densities, on the other hand, are free to assume finite values at the origin. The estimated uncertainty is not inhibited near the origin, but rather grows at a rate which depends on the absorption of the projectile wave and on the medium modifications of the effective interaction. Furthermore, orthogonality between initial and final states requires the volume integral of a monopole transition density to vanish:

$$\int dr\, r^2 \rho_0(r)=0 . \tag{14}$$

Therefore, the radial density must have at least one

node. The interior and surface lobes of the density compete for influence upon the observables. The surface lobe benefits from weaker absorption and an interaction less suppressed by density dependence. Hence, this competition tends to increase the width of the interior error envelope.

We have performed a pseudodata analysis for the lowest excited 0^+ state of ^{40}Ca, assuming that its neutron and proton densities are equal. The proton density was obtained by unfolding the proton charge form factor from the electron scattering results of Hariher *et al.*[32] Although the uncertainty in the proton density is itself not negligible, we assume, for the purposes of this pseudodata analysis, that the proton density is known exactly and examine the sensitivity to the neutron density, holding the proton density fixed.

Pseudodata spanning the range of momentum transfer between 0.4 and 2.6 fm^{-1} in steps of 0.075 fm^{-1} were constructed with 10% random fluctuations, assuming that $\rho_n=\rho_p$. Calculations were performed for many incident proton energies between 60 and 800 MeV. To the extent that the form factor specifies the angular distribution, this procedure minimizes the trivial dependence of the analysis upon kinematics.

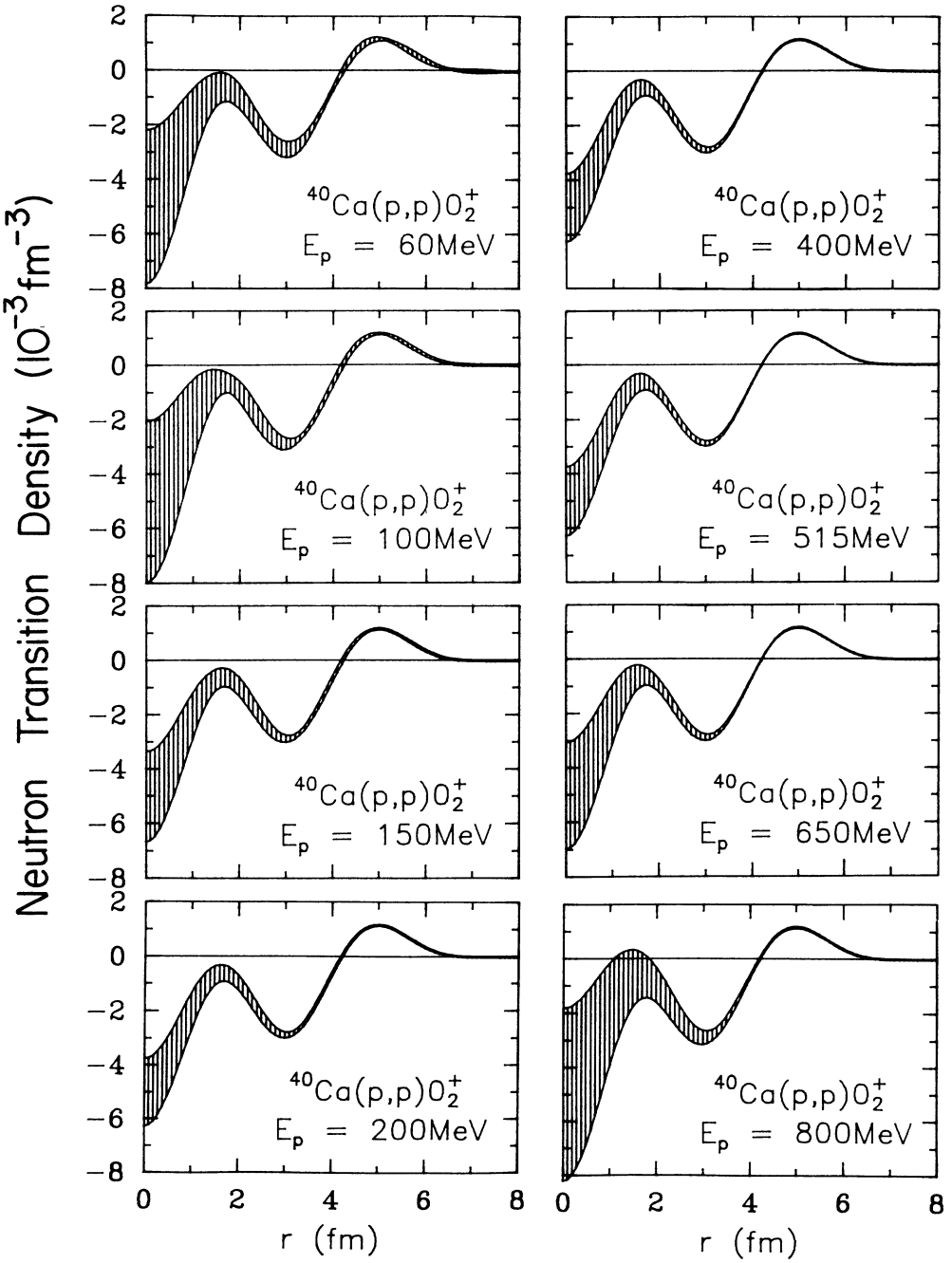

FIG. 1. Energy dependence of error envelopes for the 0_2^+ state of ^{40}Ca fitted to pseudodata for incident proton energies between 60 and 800 MeV.

The energy dependence of the radial sensitivity of proton inelastic scattering is illustrated in Fig. 1 The error envelopes for each energy were computed from the full error matrix using the FBE. For the purposes of illustration, the radial uncertainties are applied to the initial neutron density rather than to the final fitted densities. As these final densities scatter within the error bands, the differences between fitted densities complicate the comparison of the various error bands. The widths of these bands are not affected by representing the results in this way.

The surface lobes are very accurately determined for all incident energies, but the width of the error envelope increases towards the origin. The interior sensitivity appears to remain stable between 60 and 100 MeV, and then to improve rapidly between 100 and 200 MeV. The broad energy regime between about 200 and 500 MeV might be described as the *"window of visibility,"* in which the stable interior sensitivity is most nearly optimal. For higher incident energies, the error envelopes rapidly widen again as transparency is lost.

These trends are clarified by Fig. 2, which compares calculated total and absorption cross sections with the estimated uncertainty in the neutron transition density at the origin. Unfortunately, experimental data which span this entire energy regime do not appear to be available for Ca. The data complied in Refs. 33–35 for other nuclei exhibit similar energy dependencies, but our calculated cross sections seem to remain too large despite the inclusion of Pauli blocking effects. However, although the present theory is not specifically designed to provide an optimum description of integrated cross sections, it clearly does provide an adequate description of their energy dependences.

The total cross section falls rapidly below 300 MeV, whereupon the opening of the pion production channel arrests this decline and then causes the total cross section to grow again beyond 500 Mev. The energy dependence of the absorption cross section is similar, though less pronounced. Above 100 MeV, the energy dependence of the interior sensitivity is similar in form to that of the total cross section, but is even more dramatic.

Below 60 MeV, the energy dependence of the interior sensitivity is significantly different. The uncertainty at the origin is smaller at 60 MeV than it is at 100 MeV despite the large increase in total cross section between 100 and 60 MeV. The origin of this anomalous behavior is illustrated in Fig. 3, which shows the central part of the absorptive potential for several energies. For low energies, Pauli blocking substantially inhibits the growth of the absorptive potential in the interior, producing a surface-peaked potential. The reflection coefficients share this same profile as a function of classical impact parameter. Evidently, low partial waves are not absorbed as strongly as are the grazing partial waves contributing most strongly to the absorption cross section. Thus, the contribution of the interior to the inelastic differential cross section is actually somewhat larger than might be indicated by integrated cross sections alone—the radial profile must also be considered. Upon closer examination of Fig. 1, we observe that $\delta\rho_n(r)$ for 60 MeV is somewhat smaller than for 100 MeV when $r < 2$ fm, but is quite similar when $r > 2$ fm.

The relative importance of absorption and of the density dependence of the transition potential is illustrated in Fig. 4. The shaded band shows the minimum uncertainty obtained in the absence of absorption or distortion by using a density-independent interaction based on the low-density limit of the effective interaction. The intermediate band shows the effect of including inelastic density dependence while still using plane waves. Finally, the outer band includes both inelastic density dependence and the optical potential. It is clear that absorption makes the dominant contribution to the error envelope, whereas the medium modifications of the transition potential are relatively unimportant to $\delta\rho_n$. Moreover, the importance of inelastic density dependence declines rapidly with energy.

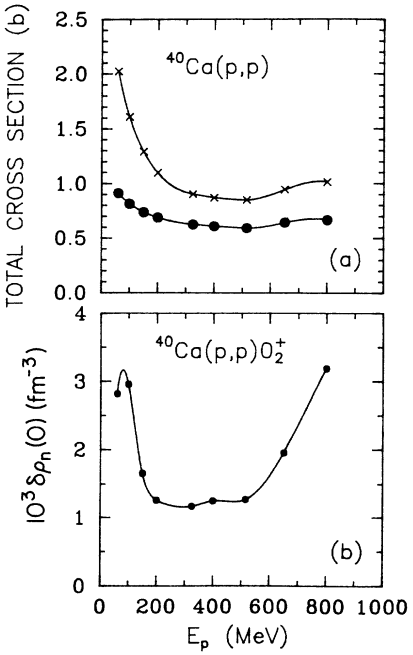

FIG. 2. (a) Energy dependence of calculated total (crosses) and absorption (circles) cross section for ^{40}Ca. (b) Statistical uncertainty in ρ_n at the origin for the 0_2^+ state of ^{40}Ca.

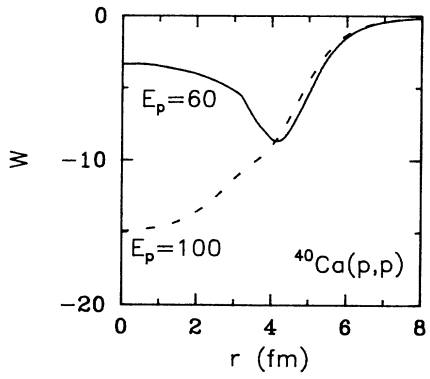

FIG. 3. Imaginary part of central optical potential for ^{40}Ca at 60 and 100 MeV.

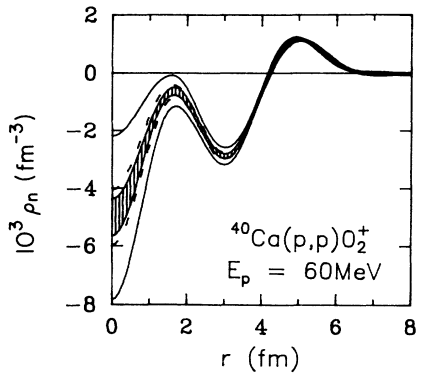

FIG. 4. Error bands for 0_2^+ neutron density of ^{40}Ca with 60 MeV protons. Inner band uses free interaction and plane waves, intermediate band (dashed lines) uses density-dependent interaction and plane waves, and outer band (solid lines) uses density-dependence interaction and distorted waves.

C. Comparison with scale-factor analyses

One often assumes that nucleon scattering is insensitive to details of the radial shape. It is then appropriate to analyze data using a single radial shape common to both neutrons and protons. This radial shape can be obtained from either the collective model or from a folding model based on the proton transition density measured by electroexcitation. Alternatively, the radial shapes can be obtained from a theoretical calculation based on the shell model. Scale factors are then fitted to the nucleon-scattering data for low momentum transfer. The results are usually reported as ratios M_n/M_p between the neutron and proton matrix elements.

However, given the radial sensitivity exhibited by the foregoing analysis, it is natural to compare the LEA with the traditional analysis for representative theoretical wave functions. To avoid confusing interaction effects with structure effects, we again employ the pseudodata method. This comparison will provide a qualitative assessment of the accuracy of scale-factor analyses for states whose neutron and proton transition densities have similar shapes in the surface region.

As a first example, we consider the 2_2^+ state of ^{34}S. This particular state is interesting because the *sd* model of Brown, Radhi, and Wildenthal[8,36] predicts a negative ratio M_n/M_p, which is unusual for low-lying normal-parity transitions. The relative sign of the neutron and proton matrix elements for this transition has been the subject of considerable controversy in recent years. Initially, Bernstein *et al.* reported that their analysis of data for 650 MeV protons confirmed the predicted negative sign.[37] However, several subsequent experiments have disputed this conclusion.[38,39] Our immediate interest in this transition concerns sensitivity to shape differences between the predicted densities and the accuracy of fitted proportionality factors.

The theory of Brown *et al.* employs a residual interaction fitted to selected energy levels throughout the *sd* shell, using an empirical dependence upon mass. Core polarization is described using the Tassie model and global effective charges. For $E2$ transitions, these effective charges are $\delta e_p = \delta e_n = 0.35\ e$. This model then yields good agreement with form factors and reduced transition probabilities for first and second 2^+ states throughout the *sd* shell. The accuracy of the neutron densities remains to be tested.

Cross section pseudodata for 200 MeV protons were produced for $q = 0.4$–2.7 fm^{-1} with $\pm 10\%$ uncertainties. Two models were then fitted to the pseudodata, as shown in Fig. 5. First, a fit using four terms of the LGE is shown as the solid line. Second, the dashed line was obtained by assuming $\rho_n \propto \rho_p$ and fitting the proportionality factor to the pseudodata for $0.6 \le q \le 1.2$ fm^{-1}. The ratio obtained by the LEA agrees with the true (input) value $M_n/M_p = -0.60$. The ratio obtained by scaling ρ_p was $M_n/M_p = -0.69$.

The scale-factor analysis provides a reasonable description of the low-q data and of the neutron density in the surface. However, the difference in shape between neutron and proton densities is clearly evident in the failure of scaling to describe the data for $q > 1.5$ fm^{-1}. Furthermore, neglect of shape differences causes a 15% error in the fitted matrix element.

Shape differences of this magnitude are commonly predicted by any semimicroscopic theory of nuclear structure. Therefore, we cannot reasonably expect better than 20% accuracy from analyses which ignore shape differences. In fact, using surveys of the neutron matrix elements fitted to hadron-scattering data for low-lying normal-parity transitions, Bernstein *et al.*[4] have concluded that an accuracy of about 20% can be expected.

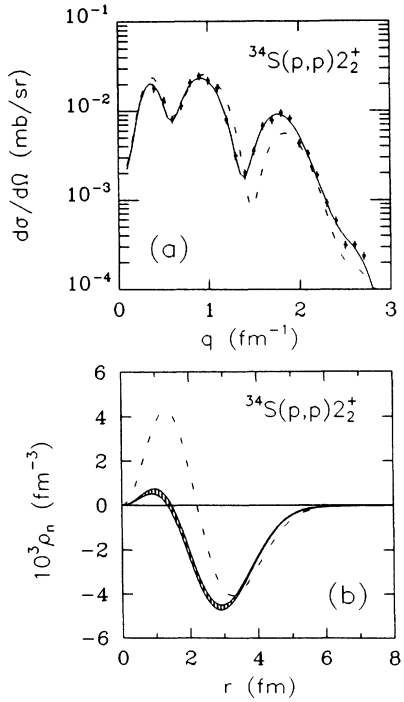

FIG. 5. (a) Pseudodata for the excitation of the 2_2^+ state of ^{34}S by 200 MeV protons. The solid line is a fit using four terms of the LGE. The dashed line, with $\rho_n = -0.69\rho_p$, was fitted to the range $0.6 \le q \le 1.2$ fm^{-1}. (b) The band represents an LGE fit to ρ_n. The dashed line portrays $\rho_n = -0.69\rho_p$.

However, this conclusion depends upon the similarity between the shapes in the surface; single-particle transitions with little core participation could easily violate this assumption.

As a second example, we consider the lowest 2^+ state of ^{206}Pb, using proton and neutron transition densities predicted by Lombard and Mas.[7] Neutron-hole transitions involving the $3p_{1/2}$ orbital provide radial distributions with considerable structure. Semiempirical coupling to giant resonances supplies the model of Lombard and Mas with enough collectivity to describe the $B(EL)$ values and form factors for low-lying 2^+ and 3^- states throughout the periodic table. Cross section pseudodata for 200 MeV protons were produced for momentum transfers between 0.25 and 2.7 fm^{-1}, in steps of 0.05 fm^{-1}, with $\pm 10\%$ uncertainties. The pseudodata were refitted using the LGE and using $\rho_n \propto \rho_p$. The same pseudodata were included in both fits. The results are shown in Fig. 6.

Although the error band estimated by the LEA does become relatively wide at the innermost lobe, considerable radial structure can still be discerned at all radii. The intrinsic radial sensitivity of intermediate-energy nucleon scattering appears adequate to probe the shape of the neutron transition density, even in the interior of large nuclei. However, the difference between the cross sections corresponding to $\rho_n = 2.6\rho_p$ and the true ρ_n are not impressive. One must have great confidence in the reaction theory to interpret deviations from proportionality that are this small. Thus, the error bands estimated by the pseudodata method must be interpreted with some care. The pseudodata approach is a closed mathematical model which estimates intrinsic radial sensitivity assuming perfect knowledge of the reaction mechanism. This approach makes no provision for systematic errors in the reaction mechanism. The effect of such errors upon the fitted density is difficult to quantify and probably cannot be faithfully represented by an error envelope.

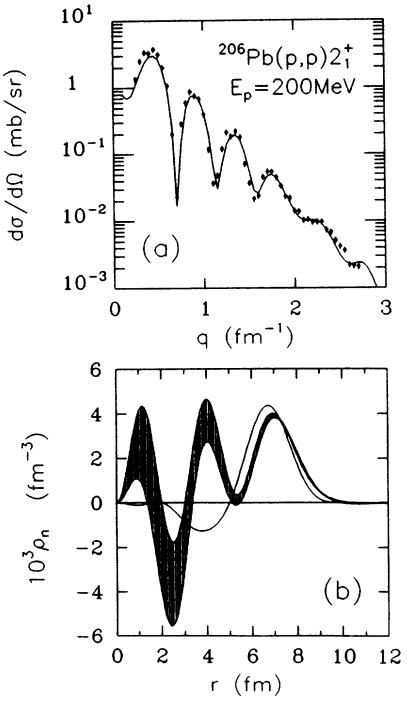

FIG. 6. (a) Pseudodata for ^{206}Pb(p,p') 2_1^+ at 200 MeV. The solid line is a scaling fit with $\rho_n = 2.6\rho_p$. The LGE fit, with $\chi_\nu^2 = 1.0$, is omitted for clarity. (b) Neutron transition densities for ^{206}Pb 2_1^+. The band was obtained by LEA, the line by scaling $\rho_n = 2.6\rho_p$.

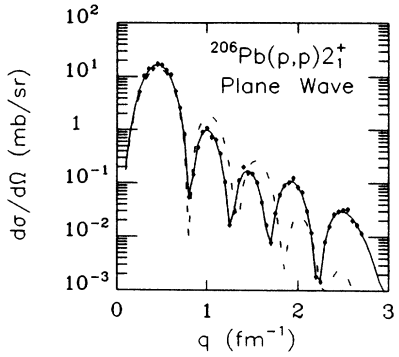

FIG. 7. Pseudodata for ^{206}Pb(p,p') 2_1^+ at 200 MeV without distortion or absorption. The solid line is an LGE fit and the dashed line represents $\rho_n = 2.6\rho_p$.

Despite the difference between the interior shapes of the two densities, the scale-factor analysis produces a fit that is pleasing to the eye. Although $\chi_\nu^2 = 6.8$ for scaling, whereas $\chi_\nu^2 = 1.05$ for the LEA, scaling would ordinarily be judged satisfactory. Evidently, the shapes of the dominant surface lobes are sufficiently similar so as to obscure the differences in interior detail. The scale-factor analysis produces an approximate fit to the surface lobe of the density, for which $M_n/M_p = 2.56$ can be compared with the correct ratio $M_n/M_p = 3.06$. The accuracy of scaling is again about 20%.

Absorption reduces the contribution of the interior relative to the surface, particularly for massive nuclei. The importance of this effect is illustrated by Fig. 7, which compares plane-wave calculations for these two models of ρ_n. The solid line represents an LGE fit, with $\chi_\nu^2 = 1.0$, to the plane-wave pseudodata. The dashed line, with $\chi_\nu^2 = 871$, results from the assumption $\rho_n = 2.6\rho_p$. Thus, we find that distortion reduces the sensitivity of χ^2 to the difference between these models by more than a factor of 100. Nevertheless, by requiring optimal χ^2, the LEA obtains a relatively narrow error envelope from the pseudodata. However, we rarely expect an optimal fit to real data. The form factor differences plainly evident in the plane-wave calculations are reduced to minor differences in detail by distortion. This problem is particularly vexing for massive nuclei. Therefore, the LEA method is most applicable to lighter nuclei with better penetrability.

D. Summary

We have investigated the intrinsic sensitivity of nucleon inelastic scattering to the radial form of the neutron transition density. The pseudodata method simulates the experimental data that would be obtained if the

best reaction model presently available were completely correct. Provided that this model describes, at least qualitatively, all important features of the interaction, the error bands deduced for fitted neutron transition densities represent the intrinsic radial sensitivity of the probe. The estimated uncertainties include the effects of absorption and density dependence in addition to the precision and range of the data. For intermediate energy nucleons, absorption makes the dominant contribution to the error envelope, whereas medium modifications of the transition potential appear to be much less important.

We have found that the intrinsic radial sensitivity of nucleon inelastic scattering is considerably better than prevailing prejudices might suggest. The intrinsic sensitivity is optimal within a broad *"window of visibility"* between about 200 and 500 MeV. The interior sensitivity is sufficient to discern radial structure even in the interior of a heavy nucleus, such as lead. Collective model and simple scaling analyses are appropriate for nucleon scattering only for highly collective excitations for which it is reasonable to assume similar shapes in the nuclear surface. Fitted scale factors then yield an estimate of M_n accurate to about 20%. For more general transitions, we must employ a method, such as the linear expansion analysis (LEA), which provides enough flexibility to describe any plausible variation of the radial density with minimal bias. The excellent radial sensitivity of nucleon inelastic scattering affords a unique and valuable opportunity to study the neutron transition density, a quantity that was previously almost completely inaccessible to detailed experimental investigation.

IV. MODEL DEPENDENCE

In principle, all expansions of the radial density based on a complete set of radial basis functions are mathematically equivalent in the sense that each is capable of reproducing any radial function that satisfies the appropriate boundary conditions. In practice, however, meaningful fits to data can only be obtained by either limiting the number of terms in the expansion or by applying physical constraints upon the coefficients. The results then become model dependent.

A fair assessment of radial sensitivity must also consider uncertainties associated with variations of the model compatible with the data but not excluded by the physical constraints. This variability represents a basic limitation upon the precision of a fitted density. Therefore, it is important to include in the error envelope an estimate of the model dependence of the fitted density.

The most important physical constraint that must be applied to the analysis describes the asymptotic behavior of the neutron form factor beyond the largest accessible momentum transfer. The implications of this constraint comprise the subject of the present section. Another important physical constraint describes the asymptotic behavior of the radial density. This constraint is relevant to the determination of radial moments, but is relegated to future publications.

A. Truncation effects

We use the lowest 2^+ state of ^{18}O to illustrate the model dependence of a fitted density. The proton density was taken from the electron scattering measurements of Norum *et al.*,[40] which extend to a maximum momentum transfer of 2.7 fm^{-1}. A neutron density was fitted to 135 MeV proton scattering data,[13] using data in the same range of q. Four terms of the PGE were used in this analysis. Rather than cloud the present analysis with peripheral issues concerning the accuracy of this result, we shall use these densities to produce pseudodata which are free of such concerns. These pseudodata were produced for $0.4 \leq q \leq 2.7$ fm^{-1} in steps of 0.1 fm^{-1} with random fluctuations corresponding to $\pm 5\%$ uncertainties in cross section.

We employ the Fourier-Bessel expansion, with a cutoff radius of 8.0 fm, to analyze the pseudodata. The effect of a finite span of momentum transfer upon the fitted density is illustrated in Fig. 8, which compares fits using six, seven, and eight terms of the FBE. All fits were done using the same set of pseudodata and used $\rho_n = 0$ as the initial guess. It appears that six terms of the FBE are not sufficient to obtain an adequate representation of the true density, shown as the solid line, based on the PGE. This particular fit of the cross section pseudodata is unsatisfactory. The truncated expansions are not equivalent and the estimated error envelope does not encompass the true density. The addition of one more term to the expansion is sufficient to obtain a good fit and to reproduce the true density. However, although the last term has a significant effect upon the quality of the fit, it is strongly correlated with the preceding term and is only weakly determined by the data. As a result, the width of the error band grows substantially. Finally,

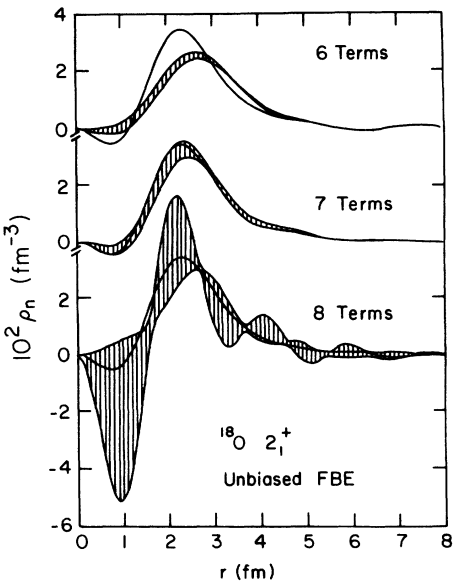

FIG. 8. Influence of the number of FBE terms in the absence of a high-q constraint. The solid line is a PGE density used to construct pseudodata. The bands portray FBE fits.

the addition of yet one more term produces a catastrophic growth in the error envelope. The oscillatory structure of the error band has eight nodes and clearly reflects the final Bessel function. An unconstrained fit cannot determine the amplitude of a frequency whose primary contribution to the cross section occurs well beyond the measured range of momentum transfer. The experimental form factor is incomplete.

A solution to the incompleteness problem for electron scattering was suggested by Borysowicz and Hetherington[41] and then developed more fully by Dreher *et al.*[28] If we assume that the single-particle wave functions for the constituent nucleons can be adequately represented by the solutions to a (nonrelativistic) Schrödinger equation with a smooth well-behaved potential, the Fourier transform of the transition density $\tilde{\rho}_l(q)$ must fall at least as fast as q^{-4} for sufficiently large q. Moreover, because nuclei have a well-defined Fermi momentum, we expect that the probability of momentum transfers larger than twice the Fermi momentum will fall precipitously. Therefore, the onset of the q^{-4} asymptotic behavior probably begins soon after $2k_F \approx 2.7$ fm^{-1}. Experiments at high-energy electron accelerators usually reach this momentum transfer. In fact, using some high-q data, Heisenberg has shown that $\tilde{\rho}_l(q)$ often falls considerably faster.[1]

Therefore, the fitting procedure must constrain the asymptotic behavior of the form factor. Although the simplest method of implementing such a constraint is to truncate the expansion, we have shown that truncated expansions are often inadequate to describe some perfectly reasonable radial densities. Moreover, the data are sensitive to the truncation of the expansion. Thus, it is necessary to ascertain the degree of radial flexibility consistent with the high-q constraint.

B. Incompleteness error

The range of $\rho(r)$ that is consistent with the postulated behavior of $\tilde{\rho}(q)$ beyond the maximum measured momentum transfer q_m can be ascertained by performing fits of the data supplemented by many random sets of permissible pseudodata beyond q_m. Dreher *et al.*[28] have demonstrated that a more economical prescription produces equivalent results. The upper limit envelope can be attached at q_m using

$$\rho^{\lim}(q)=\tilde{\rho}(q_m)(q_m/q)^4 . \tag{15}$$

The analysis is formulated most clearly using the FBE. A uniform distribution of permissible $\tilde{\rho}(q)$ points can be represented by a supplemental set of pseudodata selected at the characteristic momentum transfers q_ν beyond q_m such that

$$[\delta\tilde{\rho}(q_\nu)]^2=\tfrac{1}{3}[\rho^{\lim}(q_\nu)]^2 . \tag{16b}$$

with variances

$$[\delta\tilde{\rho}(q_\nu)]^2=\tfrac{1}{3}[\rho^{\lim}(q_\nu)]^2 . \tag{16b}$$

The factor $\frac{1}{3}$ occurs because a uniform, rather than normal, distribution is assumed.

The uncertainty $\delta\rho(r)$ in the fitted density can be decomposed into a statistical contribution $(\delta\rho)_{\text{stat}}$ due to the uncertainties δy_i in the measured data $\{y_i, i=1, N_d\}$ and a model contribution $(\delta\rho)_{\text{model}}$ due to the uncertainties in the high-q pseudodata $\{y_i, i=N_d+1, N\}$ by analyzing the propagation of errors formula

$$[\delta\rho(r)]^2=\sum_{i=1}^{N}(\delta y_i)^2\left[\frac{\partial\rho(r)}{\partial y_i}\right]^2 . \tag{17}$$

If we represent the density $\rho(r)$ using a set of fitting parameters $\{a_\nu\}$, we find that

$$\frac{\partial\rho}{\partial y_i}=\sum_\nu\frac{\partial\rho}{\partial a_\nu}\frac{\partial a_\nu}{\partial y_i} . \tag{18}$$

If we denote the fit to the ith data point as $\bar{y}_i$, we find

$$\frac{\partial a_\nu}{\partial y_i}=\sum_\mu\epsilon_{\nu\mu}\frac{\partial\bar{y}_i}{\partial a_\mu}\frac{1}{(\delta y_i)^2} , \tag{19}$$

where $\epsilon=\alpha^{-1}$ is the error matrix.

The curvature matrix $\alpha_{\mu\nu}$ can be decomposed into two parts:

$$\alpha_{\mu\nu}^{\text{stat}}=\sum_{i=1}^{N_d}\frac{1}{(\delta y_i)^2}\frac{\partial\bar{y}_i}{\partial a_\mu}\frac{\partial\bar{y}_i}{\partial a_\nu} , \tag{20a}$$

$$\alpha_{\mu\nu}^{\text{model}}=\sum_{i=N_d+1}^{N}\frac{1}{(\delta y_i)^2}\frac{\partial\bar{y}_i}{\partial a_\mu}\frac{\partial\bar{y}_i}{\partial a_\nu} , \tag{20b}$$

by assigning the measured data to α^{stat} and the pseudodata to α^{model}. We can then decompose the error matrix

$$\epsilon_{\mu\nu}=\epsilon_{\mu\nu}^{\text{stat}}+\epsilon_{\mu\nu}^{\text{model}} \tag{21a}$$

using

$$\epsilon_{\mu\nu}^{\text{stat}}=\sum_{\mu'\nu'}\epsilon_{\mu\mu'}\alpha_{\mu'\nu'}^{\text{stat}}\epsilon_{\nu'\nu} , \tag{21b}$$

$$\epsilon_{\mu\nu}^{\text{model}}=\sum_{\mu'\nu'}\epsilon_{\mu\mu'}\alpha_{\mu'\nu'}^{\text{model}}\epsilon_{\nu'\nu} . \tag{21c}$$

Note that although ϵ is the inverse of α, ϵ^{stat} is not the inverse of α^{stat} when pseudodata have been included. Substituting all of this, we find

$$(\delta\rho)_{\text{stat}}^2=\sum_{\mu\nu}\frac{\partial\rho}{\partial a_\mu}\epsilon_{\mu\nu}^{\text{stat}}\frac{\partial\rho}{\partial a_\nu} , \tag{22a}$$

$$(\delta\rho)_{\text{model}}^2=\sum_{\mu\nu}\frac{\partial\rho}{\partial a_\mu}\epsilon_{\mu\nu}^{\text{model}}\frac{\partial\rho}{\partial a_\nu} . \tag{22b}$$

This analysis is not limited to the density, but applies to any function of the fitting parameters $\{a_\nu\}$.

The procedure of Dreher *et al.*[28] consists of analyzing the error matrix for an extended data set extrapolated into the unmeasured region of momentum transfer. Therefore, we call this method of regularizing the expansion and estimating the associated incompleteness error the error matrix extrapolation method. A significant advantage of this method is that it provides a realistic error band with a single fit.

C. Applications of high-q constraint

High-q regularization of the fitting process is illustrated by the fit shown in Fig. 9(a), which used 12 terms of the FBE and includes the high-q pseudodata. This fit provides a good description of the data. The 1σ error envelope encompasses the true density over most of the radial range, whereas a 2σ band contains the true density everywhere. Therefore, this method provides a realistic estimate of the uncertainty that is neither too large nor too small.

The error band is decomposed into statistical and incompleteness errors in Fig. 9(b). Improving the statistical precision of the data reduces $(\delta\rho)_{\text{stat}}$ with little change in $(\delta\rho)_{\text{model}}$, as the latter depends mainly upon the maximum momentum transfer. The incompleteness error tends to dominate near the origin, where the influence of the high-q components is largest. The total error band is wider near the origin than that obtained from the seven-term fit and is comparable elsewhere. However, unlike the unstable bands produced by unbiased fits using truncated expansions, the error band deduced from the constrained fit is stable—additional terms in the model have little effect.

Similar results have been obtained for the 2_1^+ state of ^{206}Pb, using neutron and proton densities predicted by Heisenberg[42] to produce pseudodata for the kinematics of Sec. III C. The density obtained using 14 terms of the FBE expansion, subject to the q^{-4} asymptotic constraint, is shown in Fig. 10(a). The error band is decomposed into statistical and model contributions in Fig. 10(b). The incompleteness error clearly dominates for small radii, but is important everywhere. Despite the substantially increased width of the interior error band, considerable radial structure can still be discerned, especially beyond 3 fm. Note that the incompleteness error depends on the maximum available momentum transfer, and is independent of absorption or distortion. Under similar experimental conditions, the radial sensitivity of comparable electron scattering data is little better.

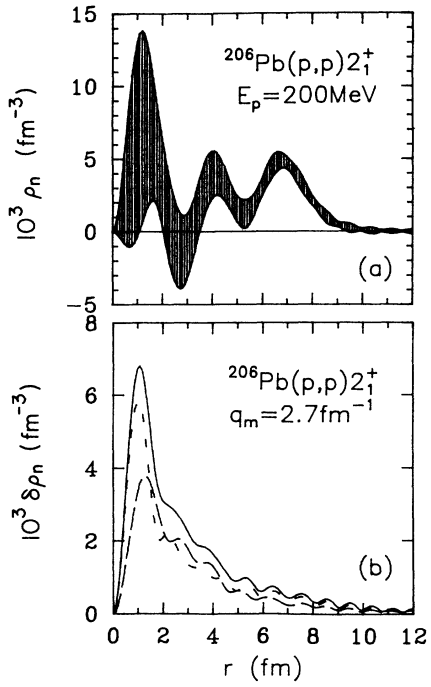

FIG. 10. (a) Neutron transition density fitted to pseudodata for the excitation of the 2_1^+ state of ^{206}Pb by 200 MeV protons; $q_m = 2.7$ fm^{-1}. (b) The total error (solid) is decomposed into statistical (long dashed) and incompleteness errors (short dashes).

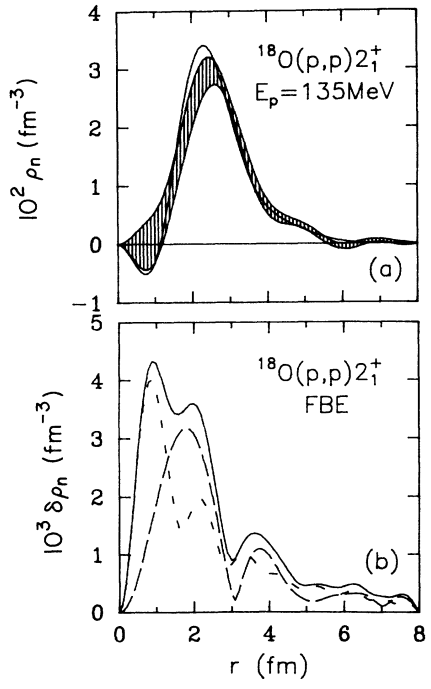

FIG. 9. (a) Density (band) fitted to pseudodata for the 2_1^+ state of ^{18}O using 12 terms of the FBE, including the high-q bias, is compared with the true density (line). (b) Statistical (long dashes) and model (short dashes) contributions to the total uncertainty (solid).

Although the statistical contribution can be reduced by improving the precision of the data, the interior incompleteness error can only be reduced by extending the measured range of momentum transfer. The strong dependence of the incompleteness error upon q_m is illustrated in Fig. 11, which shows the fitted density and error bands for the 2_1^+ state of ^{206}Pb that results when q_m is increased from 2.7 fm^{-1}, as in Fig. 10, to 3.0 fm^{-1} in Fig. 11. The incompleteness error is reduced by about a factor of 7 with this 10% increase in q_m. Much of this reduction is due to the rapid decrease in $\rho_l(q_m)$ with increasing q_m. The statistical error band is also reduced, though less strongly, by the additional data. We also note that although nucleon-scattering data can often be collected for larger momentum transfer, the sensible range for the analysis of nucleon-scattering data is usually limited by the maximum momentum transfer for which the proton density is known from electron scattering. Doubts about the reaction model for large q may also limit q_m.

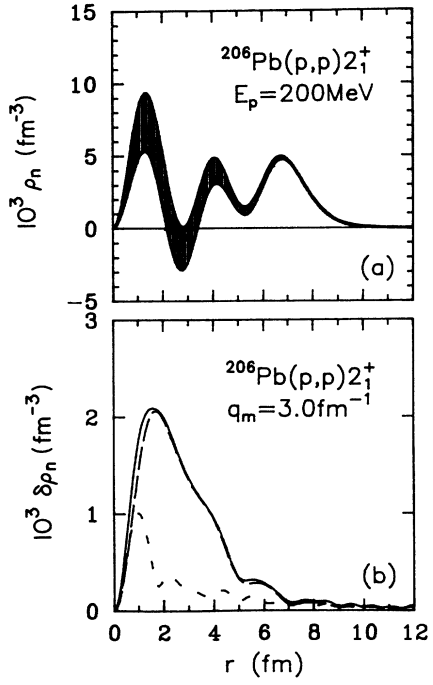

FIG. 11. (a) Neutron transition density fitted to pseudodata for the excitation of the 2_1^+ state of ^{206}Pb by 200 MeV protons; $q_m = 3.0$ fm^{-1}. (b) The total error (solid) is decomposed into statistical (long dashes) and incompleteness errors (short dashes).

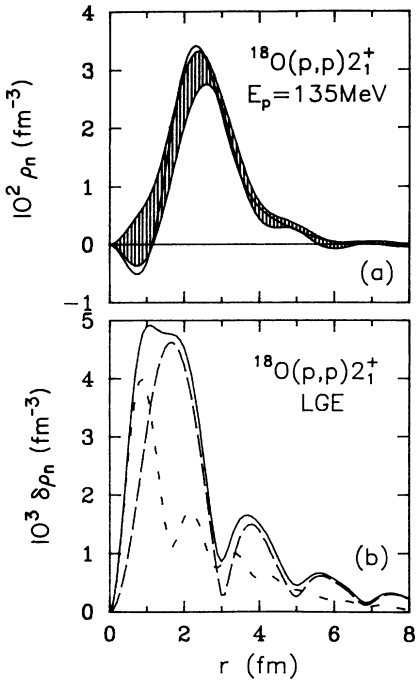

FIG. 12. (a) Density (band) fitted to pseudodata for the 2_1^+ state of ^{18}O using 12 terms of the LGE, including the high-q bias, is compared with the true density (line). (b) Statistical (long dashes) and model (short dashes) contributions to the total uncertainty (solid).

D. High-q constraint on LGE

The high-q constraint minimizes the dependence of the fitted density upon the expansion chosen to represent the density. Although the most transparent formulation of this constraint is based on the FBE, it can be applied to other expansions with similar results if the high-q pseudodata are chosen properly. For example, the nth term of the LGE yields a form factor with $(n+1)$ maxima followed by a Gaussian decline. To apply the constraint over a specified range of momentum transfer, enough terms must be included so that the last maximum of the highest term lies near the end of this range. It is usually necessary to include more terms of the LGE than of the FBE to cover the same range of momentum transfer. The absence of localization in q suggests that the pseudodata should be evenly spaced beyond q_m. However, if this spacing is too close, the constraint will be overemphasized and will reduce the estimated incompleteness error. The spacing can be decided by using a criterion based on the largest radius at which it is plausible to find an appreciable density. An extended object of characteristic radius R can only support frequencies with half-period $\Delta q \gtrsim \pi/R$. This radius should be several times the root-mean-square radius of the ground state. In the case of the oxygen isotopes, we have found that $R = 8.0$ fm is adequate to reproduce the inelastic form factors observed with electron scattering. This radius is about 3 times the rms radius of the ground state. Therefore, we expect that $\Delta q \gtrsim 0.4$ fm^{-1} is sufficient to describe the high-q behavior. This spacing is approximately the same as that between the q_ν of the FBE for large ν.

The results of applying this criterion to the high-q bias upon the LGE fit of the pseudodata for the lowest 2^+ state of ^{18}O are shown in Fig. 12. The LGE produces the same fit and yields estimates of the incompleteness and statistical uncertainties which are similar to those that emerge from the FBE. Therefore, this high-q regularization procedure minimizes the model dependence of the fitted density, while retaining sufficient flexibility to describe any physically plausible radial variation.

E. Error matrix extrapolation

Several objections have been raised to the error matrix extrapolation method. Sick contends that the practice of producing pseudodata with $\tilde{\rho}_l(q_\nu)=0$ tends to suppress oscillations of $\tilde{\rho}_l(q)$ beyond q_m more strongly than is required by the postulated asymptotic behavior, and thus underestimates the incompleteness error.[43] Furthermore, observing that the contribution to χ^2 made by pseudodata for $q > q_m$ tends to be much less than 1 per point, he also contends that the incompleteness error should be increased accordingly.[43] However, these arguments are specious because the pseudodata are drawn from a uniform, rather than from a normal, distribution.

We have demonstrated that the error matrix extrapolation procedure faithfully represents the postulated distribution, despite its relationship to χ^2, using the follow-

ing multiple trial procedure. Pseudodata with ±10% uncertainties were constructed for momentum transfers between 0.25 and 2.7 fm^{-1} in steps of 0.05 fm^{-1} using the first 10 coefficients of the FBE for the excitation of the lowest 2^+ state of ^{206}Pb by 200 MeV protons. Using a cutoff radius of 12 fm, the first 10 q_ν lie below 2.7 fm^{-1}. Independent sets of pseudodata were fit for 100 trials. After each fit, the next four coefficients were selected, at random, within the q^{-4} upper limit envelope matched to the fit at $q_m = 2.7$ fm^{-1}. These randomized coefficients describe a random modulation of the fitted density limited in amplitude by the postulated asymptotic behavior of $\tilde{\rho}_l(q)$. The density calculated from each expanded set of coefficients was then used to calculate the sample variance at each radial point.

The scatter in these densities was, of course, outside the statistical error band. However, as shown in Fig. 13, the sample variance for 100 trials agreed very well with the error band that results from the error matrix extrapolation procedure. Although the variance has almost converged after 100 trials, the fitted density has not yet quite converged to the true density—the convergence is relatively slow when the uncertainty is this large. When analyzing real data, we do not have the opportunity to evaluate a hundred or more independent trials. Furthermore, we need not include many independent sets of pseudodata or random coefficients because the error matrix extrapolation method provides the same incompleteness error in a single calculation.

Therefore, we conclude that the error matrix extrapolation method faithfully, and economically, describes the uncertainties consistent with the assumption that no more than an upper limit upon the form factor is known beyond the maximum measured momentum transfer q_m. In the absence of further knowledge, the quoted density has minimal high-q structure, but its estimated uncertainty accommodates the distribution of densities compatible with a uniform distribution of form factors beyond q_m within the upper limit envelope.

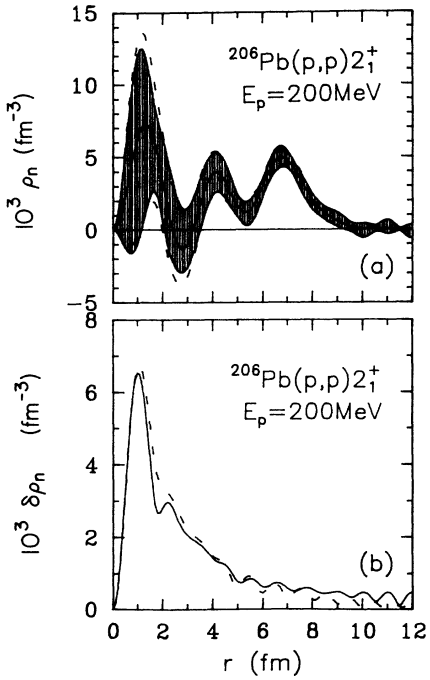

FIG. 13. (a) Average density fitted to 100 trials (band) is compared with true density (solid line) and its estimated uncertainty (dashed lines). (b) Sample variance (solid) is compared with the uncertainty estimated using the extrapolation method (dashes).

F. Asymptotic behavior

The appropriate asymptotic behavior of the form factor is still subject to some degree of ambiguity. Most notably, the procedure for matching the asymptotic tail onto the measured data is somewhat arbitrary. In comparable analyses of electron scattering data,[1] it has become customary to match the asymptotic tail onto the last measured maximum of the form factor. While this procedure may be appropriate for heavy nuclei whose form factors exhibit several maxima within the accessible range of momentum transfer, it is not appropriate for light nuclei whose form factors may exhibit only one maximum. It is then more appropriate to apply the matching condition at the largest measured momentum transfer, as prescribed by Eq. (15). In any case, it is clear that the amplitude of the asymptotic tail is somewhat arbitrary and that the estimated incompleteness error scales with this amplitude. Nevertheless, any reasonable prescription for this amplitude is sufficient to limit the unmeasurable coefficients and to thereby regularize the fitting procedure.

We also note that electromagnetic form factors measured for large momentum transfer tend to fall considerably faster than q^{-4}. Thus, it is common for electron scattering data to be analyzed assuming a considerably more restrictive exponential behavior beyond q_m.[1] Given identical match points, the incompleteness error estimated using an exponential envelope is considerably smaller than that obtained using the q^{-4} envelope. Especially in view of the ambiguities associated with the matching criterion, we believe that our criterion combined with generous error bars based upon the q^{-4} asymptotic behavior represents a suitable compromise and a realistic estimate of the incompleteness error.

V. CONCLUSIONS

The radial structure of neutron contributions to inelastic transitions is, as yet, largely unexplored. We have become accustomed, in the last decade or so, to the precision and accuracy with which electromagnetic probes view the spatial distributions of charge and current in the nucleus. With the advent of accurate high-resolution experiments using intermediate-energy protons and pions, considerable attention has been paid to nuclear structure applications which exploit the complementarity between hadronic and electromagnetic reactions. Of particular interest is the possibility of unfolding the neutron contribution to a nuclear transition whose proton density has been measured using electron

scattering. However, most analyses of hadron inelastic scattering have been content to extract from the data only a scale factor which characterizes, in a qualitative manner, the relative contributions of neutrons compared with protons.

We have developed a method for modeling direct reactions using a linear expansion analysis (LEA) of the transition amplitude. The folding model, which represents this amplitude by the "$t\rho$" convolution of an effective interaction t with a nuclear transition density ρ, is most amenable to such an approach. States of known structure can be used to calibrate an empirical effective interaction and to assess the consistency of a reaction theory. Once the interaction is known, the structure of other transitions can be investigated.

Using a pseudodata technique that is largely independent of residual inaccuracies in the reaction model, we have demonstrated that the intrinsic sensitivity of intermediate energy protons to the neutron transition density is surprisingly good, even in the interior of a large nucleus. The intrinsic sensitivity is optimal between about 200 and 500 MeV, and remains quite adequate even at 800 MeV.

When both neutron and proton transition densities peak in the nuclear surface, we find that analyses of nucleon scattering data which presuppose proportionality between neutron and proton densities or which scale shell-model wave functions yield M_n/M_p ratios accurate to about 20%. However, a scale-factor analysis is not appropriate for less collective transitions which exhibit larger shape differences. If we are to minimize the inherent bias of our analysis, we should employ a linear expansion in terms of radial basis functions drawn from a complete set.

We conclude that the excellent radial sensitivity of intermediate energy nucleon scattering is best exploited by a linear expansion analysis which extracts detailed radial information from the data with minimum bias.

ACKNOWLEDGMENTS

We thank Prof. F. W. Hersman and Prof. J. Heisenberg for supplying densities for ^{206}Pb. We also thank Prof. A. M. Bernstein and Dr. J. A. Carr for valuable criticisms of the manuscript. This work was supported by the National Science Foundation (Grant PHY-8317437).

[1] J. Heisenberg, Adv. Nucl. Phys. **12**, 61 (1981).
[2] J. Heisenberg and H. P. Blok, Annu. Rev. Nucl. Part. Sci. **33**, 569 (1983).
[3] T. W. Donnelly and I. Sick, Rev. Mod. Phys. **56**, 461 (1984).
[4] A. M. Bernstein, V. R. Brown, and V. A. Madsen, Phys. Rev. Lett. **42**, 425 (1979); A. M. Bernstein, V. R. Brown, and V. A. Madsen, Phys. Lett. **103B**, 255 (1981).
[5] R. A. Miskimen, A. M. Bernstein, B. Quinn, S. A. Wood, M. V. Hynes, G. S. Blanpied, B. G. Ritchie, and V. R. Brown, Phys. Lett. **131B**, 26 (1983).
[6] A. M. Bernstein, V. R. Brown, and V. A. Madsen, Comments Nucl. Part. Phys. **XI**, No. 5 (1983).
[7] R. J. Lombard and D. Mas, Ann. Phys. (N.Y.) **167**, 2 (1986).
[8] B. A. Brown, R. Radhi, and B. H. Wildenthal, Phys. Rep. **101**, 313 (1983).
[9] J. J. Kelly, in *Advanced Methods in the Evaluation of Nuclear Scattering Data,* Vol. 236 of *Lecture Notes in Physics,* edited by H. J. Krappe and R. Lipperheide (Springer-Verlag, Berlin, 1985), p. 335.
[10] J. J. Kelly, in *Current Problems in Nuclear Physics,* Vol. 1 of the Hellenic Physical Society Conference Series, edited by T. Paradellis and S. Kossionides (HPS, Athens, 1986), p. 325.
[11] J. A. Carr, F. Petrovich, and J. Kelly, in *Neutron-Nucleus Collisions—A Probe of Nuclear Structure,* AIP Conf. Proc. No. 124, edited by J. Rapaport, R. W. Finlay, S. M. Grimes, and F. S. Dietrich (American Institute of Physics, New York, 1985), p. 230.
[12] J. J. Kelly, in *Nuclear Structure at High Spin, Excitatio.., and Momentum Transfer, Indiana University, 1985,* AIP Conf. Proc. No. 142, edited by Hermann Nann (American Institute of Physics, New York, 1986), p. 27.
[13] J. J. Kelly, W. Bertozzi, T. N. Buti, J. M. Finn, F. W. Hersman, M. V. Hynes, C. Hyde-Wright, B. E. Norum, A. D. Bacher, G. T. Emery, C. C. Foster, W. P. Jones, D. W. Miller, B. L. Berman, J. A. Carr, and F. Petrovich, Phys. Lett. **169B**, 157 (1986).
[14] J. J. Kelly, in *Relations Between Structure and Reactions in Nuclear Physics,* edited by D. H. Feng, M. Vallieres, and B. H. Wildenthal (World-Scientific, Singapore, 1987), p. 222.
[15] L. Ray, W. Rory Coker, and G. W. Hoffman, Phys. Rev. C **18**, 2641 (1978); L. Ray, *ibid.* **19**, 1855 (1979); G. W. Hoffman, L. Ray, M. Barlett, J. McGill, G. S. Adams, G. J. Igo, F. Irom, A. T. M. Wang, C. A. Whittin, R. L. Boudrie, J. F. Amann, C. Glashausser, N. M. Hintz, G. S. Kyle, and G. S. Blanpied, *ibid.* **21**, 1488 (1980); L. Ray and G. W. Hoffman, *ibid.* **31**, 538 (1985).
[16] E. Friedman and C. J. Batty, Phys. Rev. C **17**, 34 (1978); H. J. Gils, E. Friedman, Z. Majka, and H. Rebel, *ibid.* **21**, 1245 (1980); H. J. Gils, H. Rebel, and E. Friedman, *ibid.* **29**, 1295 (1984).
[17] W. Gyles, B. M. Barnett, R. Tacik, K. L. Erdman, R. R. Johnson, G. J. Lolos, H. Roser, K. A. Aniol, F. Entezami, E. L. Mathie, D. R. Gill, E. W. Blackmore, C. A. Wiedner, S. Martin, R. J. Sobie, and T. R. Drake, Nucl. Phys. **A439**, 598 (1985).
[18] G. G. Ohlsen, Rep. Prog. Phys. **35**, 717 (1972).
[19] F. Petrovich, J. A. Carr, R. J. Philpott, A. W. Carpenter, and J. Kelly, Phys. Lett. **165B**, 19 (1985).
[20] F. Petrovich, H. McManus, V. Madsen, and J. Atkinson, Phys. Rev. Lett. **22**, 895 (1969); W. G. Love, Nucl. Phys. **A312**, 160 (1978).
[21] F. Petrovich, R. J. Philpott, A. W. Carpenter, and J. A. Carr, Nucl. Phys. **A425**, 609 (1984).
[22] J. J. Kelly, University of Maryland Report 87-098, 1987.
[23] F. Petrovich, J. A. Carr, and J. Kelly (unpublished).
[24] H. V. Von Geramb, in *The Interaction Between Medium Energy Nucleons in Nuclei—1982,* AIP Conf. Proc. No. 97, edited by H. O. Meyer (American Institute of Physics, New York, 1983), p. 44.
[25] L. Rikus, K. Nakano, and H. V. von Geramb, Nucl. Phys. **A414**, 413 (1984).
[26] W. G. Love and M. A. Franey, Phys. Rev. C **24**, 1073 (1981).

[27]H. de Vries, C. W. de Jager, and C. de Vries, At. Data Nucl. Data Tables **36**, 495 (1987).

[28]B. Dreher, J. Friedrich, K. Merle, H. Rothhaas, and G. Lührs, Nucl. Phys. **A235**, 219 (1974).

[29]H. G. Andresen and M. Müller, in *Advanced Methods in the Evaluation of Nuclear Scattering Data,* Vol. 236 of *Lecture Notes in Physics,* edited by H. J. Krappe and R. Lipperheide (Springer-Verlag, Berlin, 1985), p. 153.

[30]J. L. Friar and J. W. Negele, Nucl. Phys. **A240**, 301 (1975); **A212**, 93 (1973).

[31]J. D. Lumpe and L. Ray, Phys. Rev. C **33**, 665 (1986).

[32]P. Harihar, Kamal K. Seth, D. Barlow, S. Iversen, M. Kaletka, H. Nann, A. Saha, Claude F. Williamson, J. W. Wong, M. Deady, and W. J. Gerace, Phys. Rev. Lett. **53**, 152 (1984).

[33]P. U. Renberg, D. F. Measday, M. Pepin, P. Schwaller, B. Favier, and C. Richard-Serre, Nucl. Phys. **A183**, 81 (1972).

[34]P. Schwaller, M. Pepin, B. Favier, C. Richard-Serre, D. F. Measday, and P. U. Renberg, Nucl. Phys. **A316**, 317 (1979).

[35]L. Ray, Phys. Rev. C **20**, 1857 (1979).

[36]B. A. Brown, B. H. Wildenthal, W. Chung, S. E. Massen, M. Bernas, A. M. Bernstein, R. Miskimen, V. R. Brown, and V. A. Madsen, Phys. Rev. C **26**, 2247 (1982).

[37]A. M. Bernstein, R. A. Miskimen, B. Quinn, S. A. Wood, M. V. Hynes, G. S. Blanpied, B. G. Ritchie, and V. R. Brown, Phys. Rev. Lett. **49**, 451 (1982).

[38]A. Saha, K. K. Seth, M. Artuso, B. Harris, R. Seth, H. Nann, and W. W. Jacobs, Phys. Rev. Lett. **52**, 1876 (1984).

[39]R. Alarcon, J. Rapaport, R. T. Kouzes, W. H. Moore, and B. A. Brown, Phys. Rev. C **31**, 697 (1985).

[40]B. E. Norum, M. V. Hynes, H. Miska, W. Bertozzi, J. Kelly, S. Kowalski, F. N. Rad, C. P. Sargent, T. Sasanuma, W. Turchinetz, and B. L. Berman, Phys. Rev. C **25**, 1778 (1982).

[41]J. Borysowicz and J. H. Hetherington, Phys. Rev. C **7**, 2293 (1973); J. H. Hetherington and J. Borysowicz, Nucl. Phys. **A219**, 221 (1974).

[42]J. Heisenberg, private communication.

[43]I. Sick, in *Advanced Methods in the Evaluation of Nuclear Scattering Data,* Vol. 236 of *Lectures Notes in Physics,* edited by H. J. Krappe and R. Lipperheide (Springer-Verlag, Berlin, 1985), p. 137.